Hydrogen/deuterium-exchange (H/D-Ex) of PPARγ LBD in the presence of various modulators

YOSHITOMO HAMURO,[1] STEPHEN J. COALES,[1] JEFFREY A. MORROW,[2] KATHLEEN S. MOLNAR,[1] STEVEN J. TUSKE,[1] MARK R. SOUTHERN,[1,3] AND PATRICK R. GRIFFIN[1,3]

[1]ExSAR Corp., Monmouth Junction, New Jersey 08852, USA
[2]Sierra Analytics Inc., Modesto, California 95355, USA

(RECEIVED January 19, 2006; FINAL REVISION May 10, 2006; ACCEPTED May 15, 2006)

Abstract

A nuclear receptor, peroxisome proliferator-activated receptor γ (PPARγ), is a ligand-dependent transcription factor involved in glucose homeostasis and adipocyte differentiation. PPARγ is the molecular target of various natural and synthetic molecules, including anti-diabetic agents such as rosiglitazone. Amide hydrogen/deuterium-exchange (H/D-Ex), coupled with proteolysis and mass spectrometry, was applied to study the dynamics of the PPARγ ligand binding domain (LBD) with or without molecules that modulate PPARγ activity. The H/D-Ex patterns of ligand-free PPARγ LBD show that the ligand binding pocket of LBD is significantly more dynamic than the rest of the LBD. Presumably, the binding pocket is intrinsically disordered in order to accommodate different ligands. The presence of two full agonists (rosiglitazone and GW1929), a partial agonist (nTZDpa), and a covalent antagonist (GW9662), changed the dynamics/conformation of PPARγ LBD and slowed the H/D exchange rate in various regions of the protein. The full agonists slowed the H/D exchange more globally and to a greater extent than the partial agonist or the antagonist, indicating that the full agonist stabilizes the PPARγ LBD more than the partial agonist or the antagonist. One interesting observation is that the two full agonists significantly stabilized helix 12 while the partial agonist and the antagonist did not perturb the H/D exchange of this region. The results showed that the change in protein dynamics induced by ligand binding may be an important factor for the activation of genes and that H/D-Ex is a useful method for analyzing the biological activity of drug leads.

Keywords: hydrogen/deuterium exchange; mass spectrometry; PPARγ; protein dynamics; nuclear receptor

Supplemental material: see www.proteinscience.org

Nuclear receptors (NRs) are a superfamily of transcriptional regulators responding to a wide range of lipophilic molecules and, as a result, modulate fundamental biological processes as diverse as cellular differentiation and metabolism (Mangelsdorf et al. 1995; Pike et al. 1999; Pissios et al. 2000; Berger et al. 2003; Farnegardh et al. 2003; Kauppi et al. 2003; Nagy and Schwabe 2004; Schwabe and Teichmann 2004). Consequently, the NRs constitute a well-established class of drug targets for the treatment of diseases arising from imbalances in cellular differentiation and metabolism (Olefsky and Saltiel 2000; Saltiel 2001).

[3]Present address: The Scripps Research Institute, Jupiter, FL 33458, USA.

Reprint requests to: Yoshitomo Hamuro, ExSAR Corp., 11 Deer Park Drive, Suite 103, Monmouth Junction, NJ 08852, USA; e-mail: yhamuro@exsar.com; fax: (732) 438-1919.

Abbreviations: DMSO, dimethylsulfoxide; DTT, dithiothreitol; EDTA, ethylenediaminetetraacetic acid; H/D-Ex, hydrogen/deuterium-exchange; KCl, potassium chloride; LBD, ligand binding domain; MS, mass spectrometry; MS/MS, tandem mass spectrometry; NaCl, sodium chloride; NR, nuclear receptor; PPAR, peroxisome proliferator-activated receptor; TCEP, Tris(2-carboxyethyl)phosphine hydrochloride; TFA, trifluoroacetic acid; Tris, Tris(hydroxymethyl) aminomethane.

Article published online ahead of print. Article and publication date are at http://www.proteinscience.org/cgi/doi/10.1110/ps.062103006.

NRs bind to DNA as hetero- or homodimers and, in association with various cofactors, regulate gene transcription. Many biochemical and biophysical studies on this class of receptors suggest that agonists or antagonists binding induce conformational changes in the ligand binding domain (LBD) (Brzozowski et al. 1997; Pike et al. 1999; Johnson et al. 2000; Berger et al. 2003; Kallenberger et al. 2003). These conformational changes have been proposed to play a key role in the biological responses of nuclear receptors (Berger et al. 2003).

Peroxisome proliferator-activated receptors (PPARs) are members of the NR superfamily and serve as key regulators of dietary fats. PPAR forms a heterodimer with retinoid X receptor (RXR) (Gampe et al. 2000; Yang et al. 2000). Upon binding to fatty acids and other ligands, the heterodimer binds DNA to regulate the expression of genes for the transport and metabolism of these molecules. PPARγ plays a major role in the regulation of glucose and lipid homeostasis and is the molecular target for the antidiabetic agent rosiglitazone (Willson et al. 2000).

Amide hydrogen/deuterium exchange (H/D-Ex), coupled with proteolysis and liquid chromatography-mass spectrometry analysis (LC-MS), is a method that has recently gained in sophistication and has been used increasingly in the analysis of protein structure/dynamics (Engen and Smith 2001; Hoofnagle et al. 2001; Hamuro et al. 2003), protein–protein interactions (Ehring 1999; Baerga-Ortiz et al. 2002), and protein–ligand interactions (Engen and Smith 2001; Hamuro et al. 2002; Englander et al. 2003; Davidson et al. 2004; Yan et al. 2004). Briefly, the H/D-Ex reaction occurs when a protein (or a protein–ligand complex) is mixed with a deuterated solvent and the amide hydrogen gradually exchanges with bulk deuterium. The amide hydrogens in dynamic regions of the protein will exchange faster with bulk deuterium than those in rigid regions. After quenching the exchange reaction with cold acidic buffer, the partially deuterated protein is digested, and changes in molecular weight of each proteolytic peptide caused by the exchange of hydrogen with deuterium are measured by LC-MS.

H/D-Ex is a very sensitive probe of protein conformation/dynamics, as the amide hydrogen exchange rate is most influenced by the involvement in hydrogen bonding. Conformational and/or dynamic changes can be sublocalized to the resolution of several amino acids by coupling proteolytic digestion to H/D-Ex.

Here, H/D-Ex was applied to measure the dynamics of PPARγ LBD in the presence or the absence of various biological modulators. Our results showed that in ligand-free form, the PPARγ LBD portion proximal to the binding cavity is more dynamic than the rest of the protein. Also, the presence of full agonists rosiglitazone and GW1929 made the LBD significantly less dynamic than antagonist GW9662 and partial agonist nTZDpa.

Results

PPARγ LBD proteolytic fragmentation

Prior to H/D-Ex experiments, digestion conditions that produced PPARγ LBD fragments of optimal size and distribution for exchange analysis were established (see Materials and Methods). Pepsin digestion of PPARγ LBD was carried out by diluting the deuterated sample (1:1.5) with cold quench solution (2 M urea, 1 M TCEP at pH 2.5). The quenched sample was then passed over an immobilized pepsin column (104-μL bed volume) at a flow rate of 200 μL/min at 1°C, with a digestion time of 31 sec. These conditions generated 49 peptides covering 98% of the amino acid sequence of PPARγ LBD (Fig. 1). Twenty-three of the identified peptides that spanned 97% of the sequence were of high enough quality (high signal/noise) for H/D-Ex analysis of the PPARγ LBD (Table 1).

H/D-Ex of ligand-free PPARγ LBD

Ligand-free PPARγ LBD was incubated in deuterated Tris buffer (pH 8.0) for 30–10,000 sec at 25 ± 1°C. After

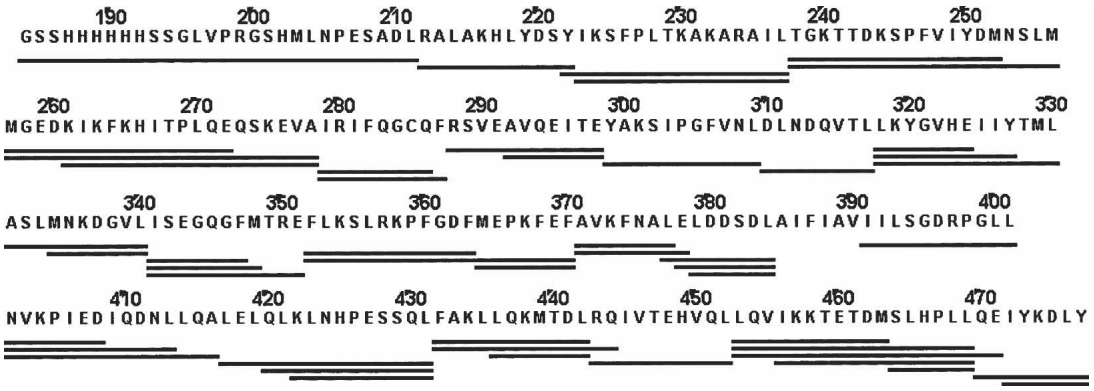

Figure 1. Pepsin digest peptide coverage map of PPARγ LBD. Bold lines indicate the peptide fragments identified.

Table 1. *Average deuteration level of each segment in apo PPARγ LBD and average difference in deuteration levels of PPARγ LBD with or without various modulators*

Structure[a]	Residues[b]		Charge[c]	apo[d]	GW9662[e]	nTZDpa[e]	GW1929[e]	rosi[e]
–H1	186	211	3	103%	0%	0%	1%	1%
H1	214	222	2	27%	−3%	6%	−1%	0%
H2	225	237	2	72%	−6%	4%	**−14%**	−7%
H2′	240	256	2	96%	−3%	−4%	3%	−5%
H2′– H3	259	278	2	101%	1%	0%	0%	0%
H3	281	287	1	100%	N.A.	**−29%**	**−72%**	**−40%**
H3	290	298	1	83%	**−41%**	**−47%**	**−72%**	**−52%**
H3′	301	309	1	23%	−3%	1%	−2%	1%
H4	312	317	1	24%	0%	1%	−2%	0%
H5	320	327	1	14%	−5%	−4%	−8%	−9%
H5–H6	333	340	1	47%	**−16%**	−7%	**−25%**	**−24%**
H6	343	351	1	82%	**−11%**	**−21%**	**−24%**	**−26%**
H6–H7	354	363	2	77%	**−15%**	−8%	**−27%**	**−21%**
H7	366	370	1	75%	−8%	−6%	**−50%**	**−41%**
H7	373	377	1	75%	**−20%**	−6%	**−42%**	**−29%**
H8	380	384	1	56%	6%	9%	3%	1%
H8–H9	393	401	1	51%	−6%	0%	−2%	−2%
H9	404	416	2	7%	1%	−4%	0%	4%
H9–H10	419	431	2	52%	−2%	3%	−1%	0%
H10	434	442	2	47%	−9%	1%	−2%	−1%
H11	445	452	2	76%	3%	−2%	**−58%**	**−50%**
H11–H12	455	469	2	97%	−1%	0%	**−12%**	−8%
H12–	472	477	1	97%	−1%	−1%	**−22%**	**−19%**

A negative number indicates that the segment exchanges slower with the ligand. A positive number indicates that the segment exchanges faster with the ligand. A bold number indicates that the average difference is >10%, which is considered a significant change.
[a] Structure indicates the structural element of each segment.
[b] Residue numbers are adjusted to the full-length PPARγ residue numbers.
[c] Charge is the charge state of each peptide observed.
[d] Apo is the average deuteration level of each segment in apo PPARγ LBD.
[e] The other columns are the average difference in deuteration levels of PPARγ LBD with or without each ligand.

the incubation, the exchange reaction was quenched with 2 M urea, 1 M TCEP (pH 2.5) at 1°C. As the amide hydrogen exchange reaction at neutral pH is primarily base-catalyzed, low temperature and low pH slow down the exchange rate significantly. However, because the digestion and separation steps are in an aqueous environment, a small percentage of amide deuterium gradually reverts back to hydrogen. The average deuterium retention during the analysis was measured to be 68% (see Materials and Methods).

The deuteration level of ligand-free PPARγ LBD as a function of incubation time is illustrated in Figure 2. Each block in the figure represents one of the 23 high-quality peptides, and each block contains six time points ([from top] 30, 100, 300, 1000, 3000, and 10,000 sec). In this figure, dynamic and fast exchanging segments are shown in red, while ordered and slow exchanging segments are shown in blue. Slow exchanging regions, where the average deuteration level of the aforementioned six time points is <50%, include segments 214–222 (helix 1), 301–309 (helix 3′), 312–317 (helix 4), 320–327 (helix 5), 333–340 (between helices 5 and 6), 404–416 (helix 9), and 434–442 (helix 10). Fast exchanging segments, where the average deuteration level is >90%, include 240–256 (helix 2′), 259–278 (between helices 2′ and 3), 281–287 (helix 3), 455–469 (between helices 11 and 12), and 472–477 (helix 12). Finally, some segments exchange at intermediate rates, specifically helices 2, 6, 7, 8, and 11 (see also Table 1).

The dynamic properties of the PPARγ LBD became apparent when the H/D-Ex results were overlaid onto the three-dimensional X-ray crystal structure of PPARγ LBD (Fig. 3A). The H/D-Ex results varied greatly between distinct regions of the LBD domain. For clarity, three subdomains are defined: upper (H1, H3′, H4, H5, between H5 and H6, H9, H10), intermediate (H2, H6, H7, H8, H11), and lower (H2′, between H2′ and H3, H3, between H11 and H12, H12). While the upper subdomain in the LBD (Fig. 3A) exchanges slowly, the intermediate and the lower subdomains of the LBD exchange faster, suggesting that the binding cavity located in the lower subdomain of LBD is more dynamic than the rest of the domain. The lower subdomain may be intrinsically disordered to accommodate various ligands (Wright and Dyson 1999). This observation is consistent with the crystallographic temperature factor analysis (Nolte et al. 1998; Nagy and Schwabe 2004) and the NMR cross-peak

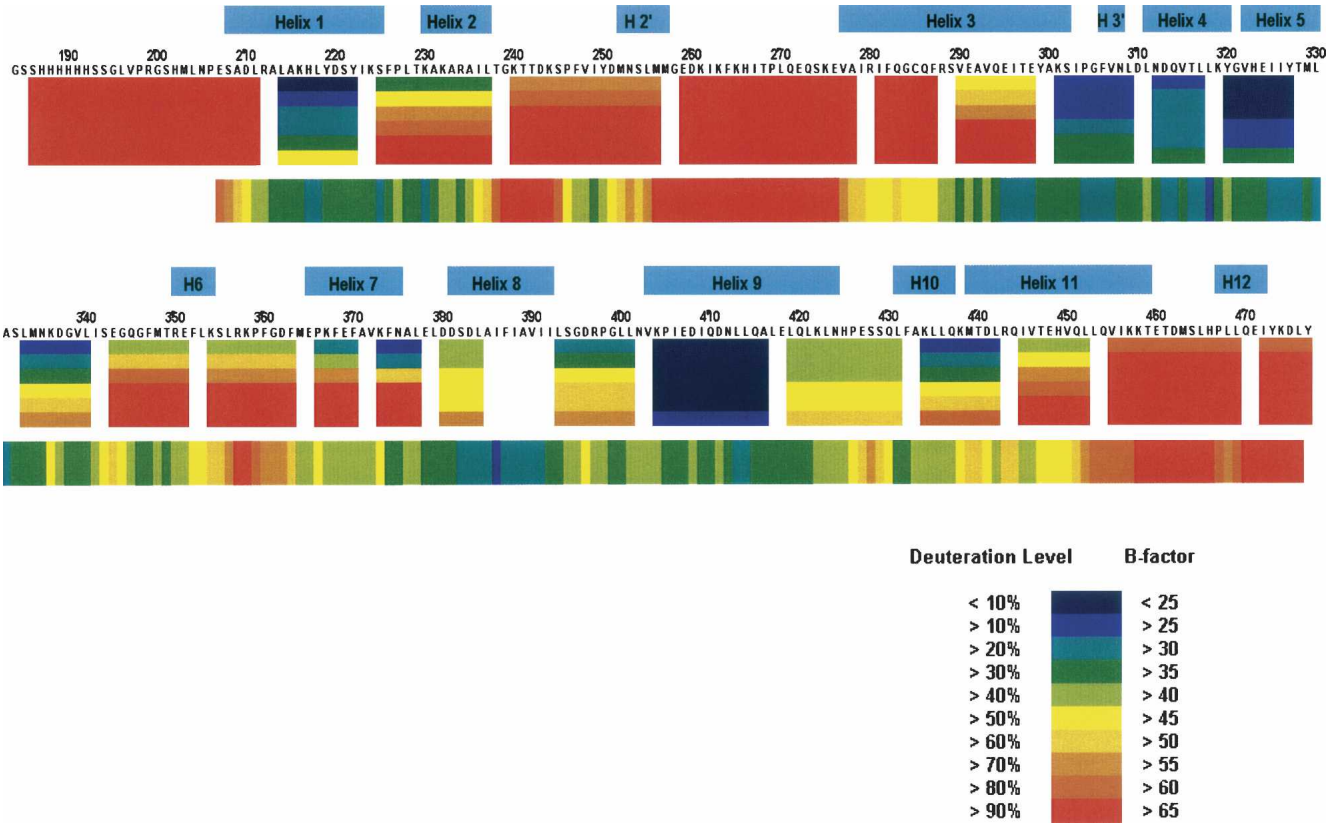

Figure 2. H/D-Ex pattern of PPARγ LBD without ligands. Each horizontal color block represents an analyzed peptic peptide, and each block contains six time points ([from *top*] 30, 100, 300, 1000, 3000, and 10,000 sec). The deuteration level of each peptide at each time point is color-coded (see *bottom right*). The first two residues of each peptide lose the deuterium during analysis (Bai et al. 1993). Therefore, for example, the information obtained from peptide 184–211 is actually the information on residues 186–211. This also accounts for the two-residue gaps between peptides. The vertical color blocks at the *bottom* represent the *B*-factor of apo PPARγ LBD (1PRG) and correspond to the same color-coded key at the *bottom right*.

analysis (Johnson et al. 2000). The crystallographic temperature factors of the upper subdomain of LBD were lower, while those of the lower subdomain were higher (Fig. 3B; Nolte et al. 1998; Nagy and Schwabe 2004). While the three-dimensional NMR cross-peaks at the upper subdomain of PPARγ LBD were sharp, those at the lower subdomain were broad, indicating a very dynamic character for this region of the LBD (Johnson et al. 2000).

H/D-Ex perturbations of PPARγ LBD by various modulators

The H/D-Ex perturbations of PPARγ LBD in the presence of various modulators were measured. The modulators used in this study are antagonist GW9662 (Leesnitzer et al. 2002), partial agonist nTZDpa (Berger et al. 2003), and two full agonists, GW1929 (Brown et al. 1999) and rosiglitazone (Nolte et al. 1998) (Fig. 4). All four PPARγ LBD–ligand complex solutions were added to deuterated water, and the mixture was incubated in an analogous manner as ligand-free PPARγ LBD (see Materials and Methods). Each of the modulators perturbed the PPARγ LBD to a different degree (Fig. 5). The dark blue regions indicate no difference in deuteration with or without ligand. The regions containing the remainder of the color spectrum indicate different degrees to which the ligands protected PPARγ LBD from deuteration. The regions protected by rosiglitazone coincide with known PPARγ LBD–rosiglitazone contact residues (Fig. 5, red circles). The average difference in deuteration levels among six time points for each segment with each ligand is summarized in Table 1.

Two full agonists, GW1929 and rosiglitazone, perturbed the H/D-Ex of PPARγ LBD broadly and similarly. Both ligands slowed the H/D exchange of segments 281–287 (helix 3), 290–298 (helix 3), 333–340 (between helices 5 and 6), 343–351 (helix 6), 354–363 (between helices 6 and 7), 366–370 (helix 7), 373–377 (helix 7), 445–452 (helix 11), and 472–477 (helix 12). The effect was so broad that it appeared as if the entire binding cavity became rigid upon binding full agonists.

On the other hand, the perturbations by antagonist (GW9662) or partial agonist (nTZDpa) were more localized.

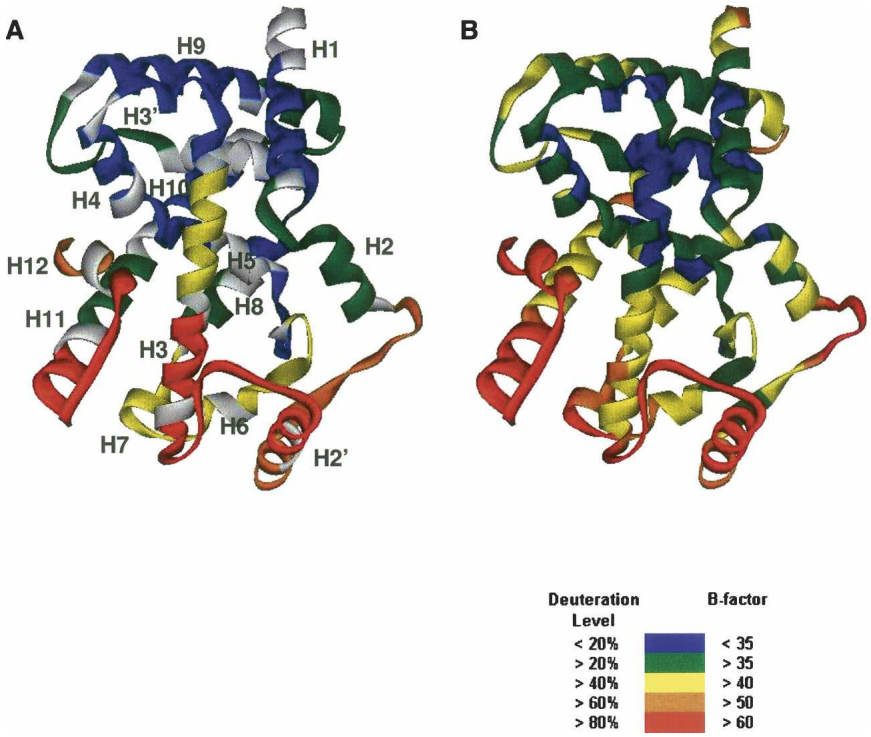

Figure 3. (*A*) H/D-Ex results (300-sec exchange) overlaid onto a three-dimensional crystallographic structure of PPARγ LBD. The deuteration level at this time point is color-coded at *bottom right*. Gray is the region not covered by the current experimental set. The primary reason for a gray gap is mentioned in the Figure 2 legend. (*B*) *B*-factor of apo PPARγ LBD (1PRG).

GW9662 slowed the H/D exchange of segments 290–298 (helix 3), 333–340 (between helices 5 and 6), 343–351 (helix 6), 354–363 (between helices 6 and 7), and 373–377 (helix 7). nTZDpa had the narrowest perturbation, only slowing H/D exchange of the segments 281–287 (helix 3), 290–298 (helix 3), and 343–351 (helix 6).

One striking variation in the H/D exchange of PPARγ LBD with these ligands is the perturbations at the C terminus. The two full agonists slowed exchange at helix 11 (445–451) and helix 12 (472–477), while the antagonist and the partial agonist did not have any effect on these regions (Figs. 6, 7). The alignment of helix 12 has been implicated to play a critical role in transcriptional activation.

All four ligands tested significantly perturbed segment 290–298, which is the C-terminal half of helix 3. Three ligands—nTZDpa, GW1929, and rosiglitazone—also slowed down exchange of segment 281–287 covering the other half of helix 3. This peptide was not observed in the experiments with GW9662, due to the covalent modification at cysteine 313.

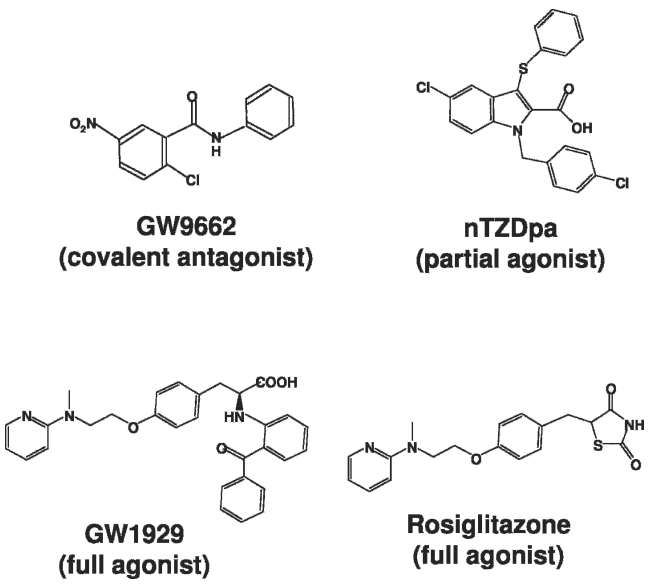

Figure 4. Structures of PPARγ ligands.

Discussion

Correlation between H/D-Ex results and X-ray B*-factor*

The rate of amide hydrogen exchange is dependent upon local fluctuations in protein structure (Englander and Kallenbach 1984). For this reason the rate of H/D-Ex is a good indicator of regional flexibility within a protein.

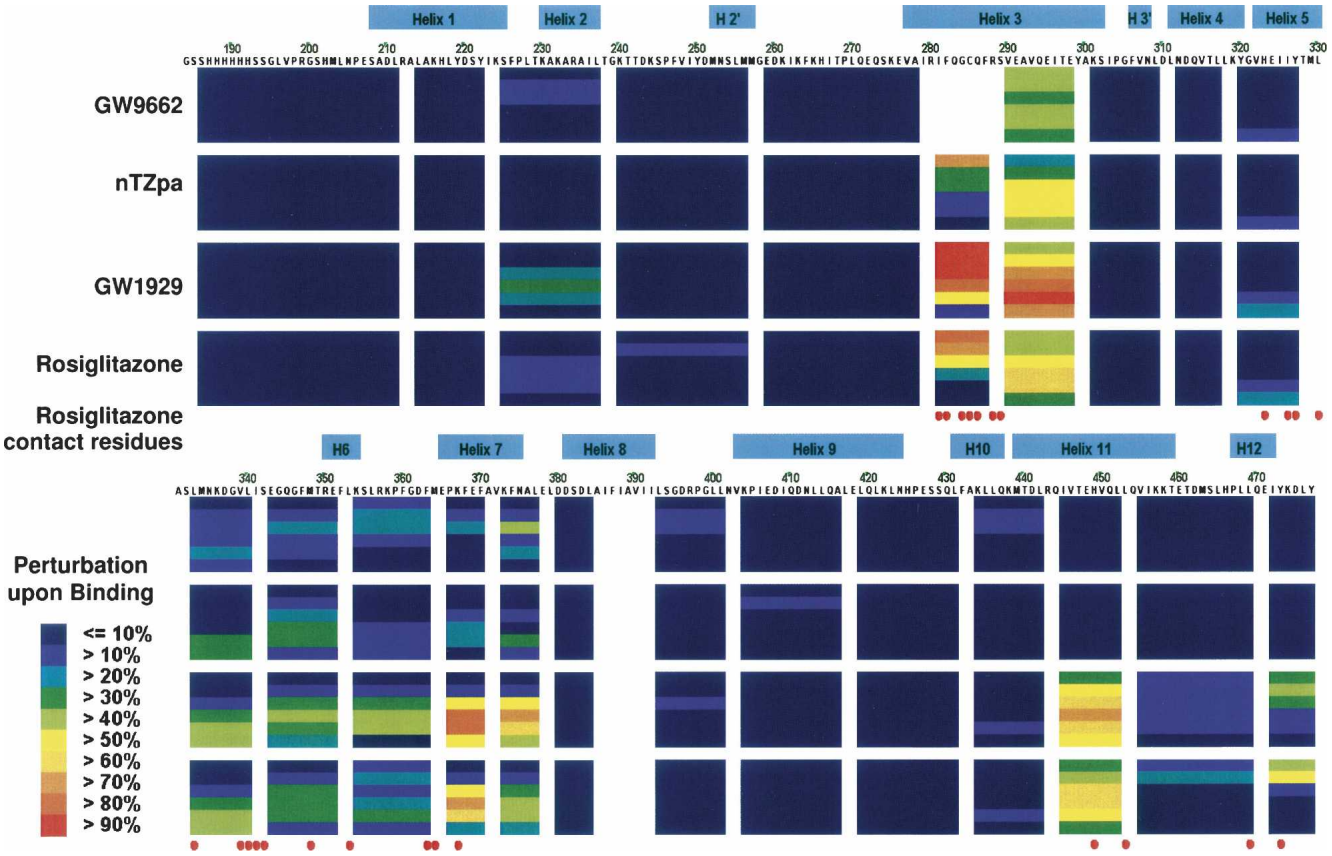

Figure 5. H/D-Ex perturbations upon ligand binding. The figure shows the difference of deuteration levels with or without each ligand. Dark blue indicates no change in deuteration level upon ligand binding. Other colors indicate the changes upon ligand binding (see *bottom left*). The red circles *below* the H/D-Ex perturbation indicate the residues that are identified from the crystal structure as contact residues between PPARγ LBD and roziglitazone.

The atomic temperature factor (*B*-factor) reflects the mobility of an atom in an X-ray crystal structure. It is therefore reasonable to expect that a correlation between B-factor and rates of H/D-Ex should exist (Kossiakoff 1982; Zhang et al. 1996).

In the present study on the dynamics of PPARγ LBD, the H/D-Ex protection factor (the retardation of amide hydrogen exchange rate upon folding) for each segment in ligand-free PPARγ LBD was calculated (see Supplemental Material). The *B*-factors for main-chain atoms for both molecules of PPARγ LBD in the asymmetric unit (1PRG) were averaged. The correlation between the H/D-Ex protection factors and the average *B*-factors was plotted (Fig. 8).

There is a moderate correlation ($R^2 = 0.69$) between the logarithm of the H/D-Ex protection factor and the crystallographic *B*-factors (Fig. 8). The reasons for this moderate correlation can be explained by one or more of the following: (1) H/D-Ex represents protein dynamics in solution, whereas the *B*-factor values represent dynamics in the solid state. Regions that can move freely in solution may be constrained by contacts within the crystal lattice. For PPARγ LBD, the regions 240–256, 259–278, 281–287, 290–298, 455–469, and 472–477 have average *B*-factors lower than expected from H/D-Ex protection factors, and many of these residues participate in intermolecular contacts within the crystal lattice. In general, the PPARγ LBD crystal structure (1PRG) has tight crystal packing (45% solvent content), and some regions would therefore be less dynamic than in solution. (2) The H/D-Ex time window employed was 30–10,000 sec, and there are a few segments for which H/D-Ex occurs completely before 30 sec. The lack of shorter time points prevents accurate estimation of the exchange rates in these segments. (3) The resolution limit of structural dynamics measured by H/D-Ex is a few amino acids, while *B*-factors of moderate- to high-resolution crystal structures attempt to explain the dynamics of individual atoms. Some finer correlation between protection factors and *B*-factors might have been averaged out due to this difference. David Smith and colleagues (Zhang et al. 1996) also observed a weak correlation between the log of average exchange rates and the *B*-factors for rabbit muscle aldolase. A wider time window and higher resolution

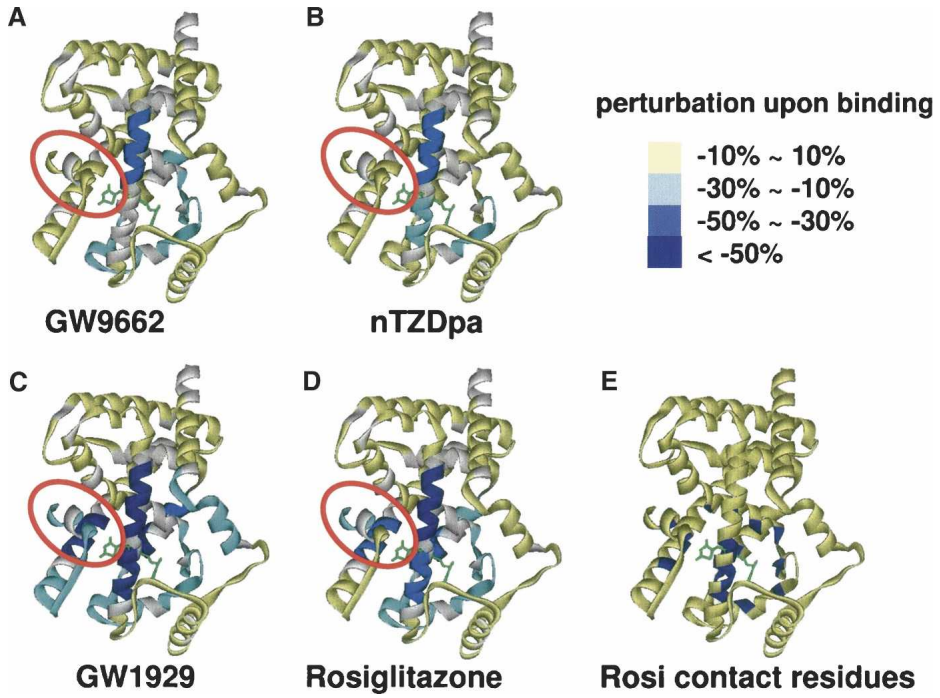

Figure 6. Average difference in deuteration levels of PPARγ LBD with or without ligands overlaid onto a three-dimensional crystallographic structure of PPARγ LBD with rosiglitazone (2PRG). Blue indicates that the segment exchanges slower with the ligand present. Yellow indicates that the segment exchanges about the same rate with or without the ligand present. Light green molecule is rosiglitazone. Gray is the region not covered by the current experimental set primarily due to the reason mentioned in the Figure 2 legend.

data may improve the correlation and/or give a clearer picture of the difference between the two observables.

Full agonists stabilize PPARγ LBD

The protease protection analysis (Berger et al. 2003) and X-ray crystallography studies of NRs revealed that the NRs change their conformations upon binding biological modulators (Nolte et al. 1998). These results indicated that the conformation of NR, especially helix 12, is critical for gene activation. Recent NMR studies by Johnson et al. (2000) suggested that not only does the PPARγ LBD undergo a conformational change, it also changes dynamically. In their study, the three-dimensional HNCO NMR cross-peaks of PPARγ LBD were well resolved in the complex with a full agonist, rosiglitazone, while the cross-peaks of the unliganded PPARγ LBD were found to be overlapping, presumably due to the increased mobility of the protein. This effect was pronounced in the lower subdomain of the LBD, especially helices 3, 5, 6, 7, 11, and 12. They proposed that a full agonist such as rosiglitazone stabilizes PPARγ LBD in the conformation favorable for cofactor binding, which also aids in the recruitment of the cofactor.

The H/D-Ex results on PPARγ LBD presented here are consistent with NMR cross-peak analysis performed on PPARγ LBD by Johnson et al. (2000). The H/D-Ex results show the lower subdomain, containing the ligand binding pocket, to be exchanging much faster in the ligand-free form than in the full agonist complexes (Fig. 6). The decrease in the exchange rate or protection upon ligand binding suggests that the local dynamics/mobility of the protein were also decreased. The amide hydrogen exchange rate is mostly influenced by backbone amide hydrogen bonding; therefore, the changes in the rate of H/D-Ex can be interpreted as conformational/dynamic perturbation upon ligand binding. The regions where the NMR cross-peaks were lost in the absence of rosiglitazone were in agreement with the regions protected from H/D-Ex in the PPARγ LBD full agonist complex.

Full agonists vs. partial agonists

PPARγ is the molecular target for compounds such as rosiglitazone and pioglitazone for the treatment of type II diabetes (Willson et al. 2000). These molecules are full agonists of PPARγ and serve to sensitize adipose tissue to insulin. While these full agonists are very efficacious, they have undesirable side effects, including edema and weight gain (Berger et al. 2003). Full agonists may lock the PPARγ into an active structural conformation, leading to broad gene regulation in adipose tissue and to the

undesired side effects. A partial agonist has been found to have a more moderate clinical profile and an advantage as a therapeutic agent because it acts upon a subset of genes regulated by the full agonist.

A partial agonist, nTZDpa, perturbed the H/D-Ex of PPARγ LBD far less than full agonists. nTZDpa protected helices 3 and 6 (Fig. 6). This is consistent with the aforementioned NMR results, which also showed very little change in the patterns of cross-peaks in the presence or the absence of nTZDpa (Berger et al. 2003).

While the crystallographic structure of PPARγ LBD in the presence of nTZDpa is not available, the co-crystal structure with the partial agonist, GW0072, is available (4PRG; Oberfield et al. 1999). One intriguing difference between this structure and rosiglitazone-bound PPARγ LBD is that a carbonyl of the thiazolidinedione group in rosiglitazone participates in a hydrogen bonding network with residues H323 (helix 5), H449 (helix 11), and Y473 (helix 12), while GW0072 is too far away to interact with these PPARγ residues. The lack of a hydrogen bonding network around helix 12 in the PPARγ LBD–partial agonist (GW0072) complex probably affords the helix 12 region greater mobility than the PPARγ LBD–rosiglitazone complex.

Antagonist GW9662

The detailed interactions between PPARγ and GW9662 are not well understood (Leesnitzer et al. 2002). The co-crystallographic structure of this complex is not available, and NMR studies have not yet been carried out for this complex. Co-crystal structures of another NR, estrogen receptor (ER), bound to agonist and antagonist, reveals that the two ligands bind at the same site while inducing distinct conformational changes in helices 11 and 12 of the LBD (Brzozowski et al. 1997). On the other hand, the co-crystal structure of glucocorticoid receptor (GR) in the presence of antagonist RU486, shows that helices 11 and 12 of GR are very flexible (Kauppi et al. 2003). The current H/D-Ex results presented here show that helices 11 and 12 of PPARγ LBD remained as dynamic as the ligand free-form when complexed with antagonist GW9662. No change in the rate of deuterium buildup near helices 11 and 12 was observed (Fig. 7). This implies that, unlike full agonists, no conformational or dynamic change occurs in this region upon the antagonist binding to PPARγ. The effects were somewhat similar to the partial agonist, nTZDpa, and very different from the two full agonists studied in this work.

Nuclear receptor research and H/D-Ex

While structure-based drug discovery using X-ray crystallography is currently the most powerful approach for finding new drugs, crystallization remains a major obstacle. Certain proteins and protein–ligand complexes are inherently noncrystallizable. For NR research, crystal structures of full-length NRs remain unavailable, and the number of co-crystal structures is limited compared with the number of known drug candidates.

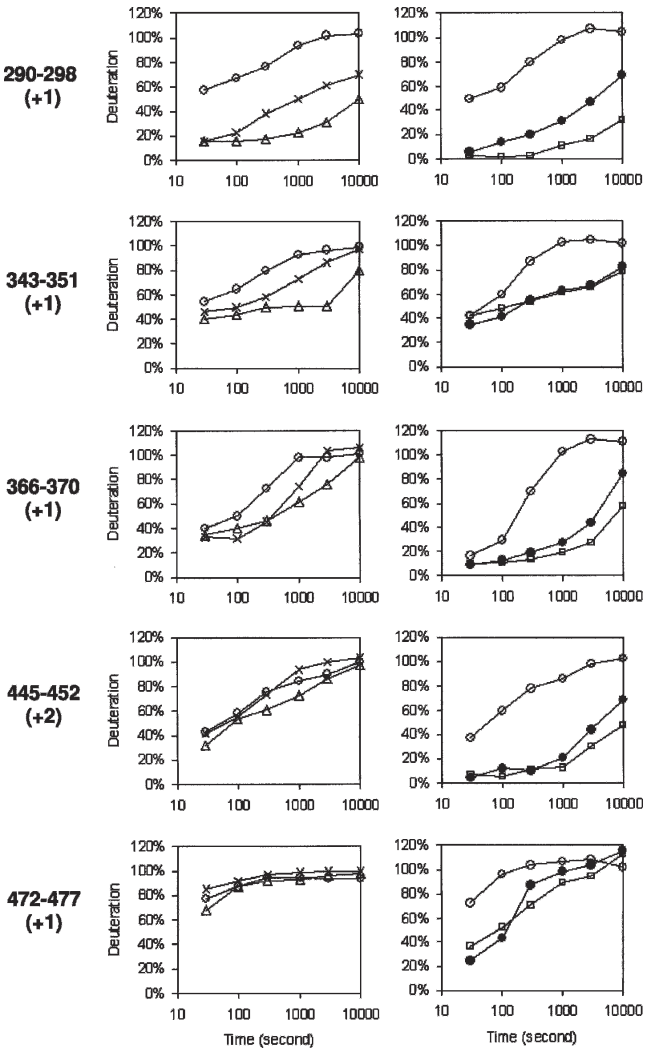

Figure 7. Deuterium content in each segment of PPARγ LBD at 30, 100, 300, 1000, 3000, and 10,000 sec with or without ligands: ligand-free (○), GW9662 (×), nTZDpa (Δ), GW1929 (□), and rosiglitazone (●).

H/D-Ex can be a powerful method for the investigation of NR structure and function, and offers information that is complementary to that gained through X-ray crystallography. It is increasingly evident that the dynamics of the LBD of NRs are very important to the mechanism of NR function (Nagy and Schwabe 2004). The H/D-Ex technology can measure the dynamics of NRs at the submolecular level and in solution instead of the solid state. The technology is also applicable to full-length NRs or other ligands that may not co-crystallize with their target.

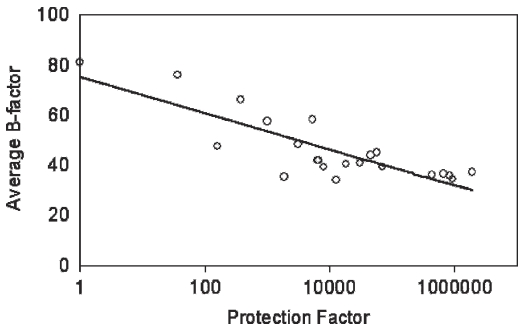

Figure 8. Correlation between the logarithm of H/D-Ex protection factor and the crystallographic *B*-factor. Each circle represents a peptic segment analyzed. *R*-square value was 0.69.

One implication of the results reported here is that H/D-Ex may be able to differentiate partial agonists from full agonists using the dynamic properties of helices 11 and 12 of PPARγ LBD.

Materials and methods

Materials

His-tagged PPARγ LBD (33 kDa, 1 mg/mL, 30 μM, 20 mM Tris, 10% glycerol, 100 mM KCl, 0.2 mM EDTA, 1 mM DTT) was purchased from ProteinOne. Poros 20 AL media for the immobilized pepsin column was purchased from Applied Biosystems. All other reagents were obtained from Sigma.

General operation procedure

A 20-μL reaction volume of H/D-exchanged protein solution was quenched by shifting to pH 2.5 with 30 μL of 2 M urea and 1 M TCEP at 1°C. The quenched solution was immediately pumped over a pepsin column (104-μL bed volume) filled with porcine pepsin (Sigma) immobilized on Poros 20 AL media at 30 mg/mL per the manufacturer's instructions (Hamuro et al. 2003), with 0.05% TFA (200 μL/min) for 3 min with a contemporaneous collection of proteolytic products by a trap column (4-μL bed volume). Subsequently, the peptide fragments were eluted from the trap column and separated by a C18 column (Magic C18, Michrom BioResources, Inc.) with a linear gradient of 15% solvent B to 40% solvent B over 23 min (solvent A, 0.05% TFA in water; solvent B, 80% acetonitrile, 20% water, 0.01% TFA; flow rate 5–10 μL/min). Mass spectrometric analyses were carried out with a Thermo Finnigan LCQ mass spectrometer (Thermo Electron Corp.) with capillary temperature at 200°C.

Sequence identification of pepsin-generated peptides

To quickly identify pepsin-generated peptides for each digestion condition employed, spectral data were acquired in data-dependent MS/MS mode with dynamic exclusion. The SEQUEST software program (Thermo Electron Corp.) was used to identify the sequence of the dynamically selected parent peptide ions. This tentative peptide identification was verified by visual confirmation of the parent ion charge state presumed by the SEQUEST program for each peptide. This set of peptides was then further examined to determine if the quality of the measured isotopic envelope of peptides was sufficient to allow accurate measurement of the geometric centroid of isotopic envelopes on deuterated samples.

Hydrogen/deuterium exchange experiments

A PPARγ LBD stock solution was prepared by mixing 20 μL of 1 mg/mL His-tagged PPARγ LBD (33 kDa, 30 μM; ProteinOne) with 1.2 μL of DMSO solution (±10 mM ligand) and 18.8 μL of 20% glycerol. The stock solution was incubated at 1°C for at least 2 h prior to the initiation of H/D-Ex experiments. An exchange reaction was initiated by diluting 4 μL of PPARγ LBD stock solution (±ligand) with 16 μL of deuterated buffer (20 mM Tris, 100 mM NaCl at pH_{read} 8.0). The concentration of the protein was 3 μM, and that of ligand was 60 μM (20-fold excess) in the reaction solution, which contained 0.6% DMSO, 3% glycerol, and 80% deuterated water. The reaction mixture was incubated at 25 ± 1°C for varying times (30–10,000 sec). These partially deuterated samples were then subjected to H/D-Ex analysis as above, along with control samples of nondeuterated (ran without deuterated buffers) and fully deuterated PPARγ LBD (incubated in 80 mM TCEP in 80% D_2O for 2 d at 37°C).

The centroids of probe peptide isotopic envelopes were measured using the in-house-developed program in collaboration with Sierra Analytics. The corrections for back-exchange were made employing methods described previously (Zhang and Smith 1993):

$$\text{Deuteration level}(\%) = \frac{m(P) - m(N)}{m(F) - m(N)} \times 100$$

$$\text{Deuterium incorporation}(\#) = \frac{m(P) - m(N)}{m(F) - m(N)} \times \text{MaxD}$$

where m(P), m(N), and m(F) are the centroid value of partially deuterated peptide, nondeuterated peptide, and fully deuterated peptide, respectively. MaxD is the maximum deuterium incorporation calculated by subtracting the number of prolines in the third or later amino acid and two from the number of amino acids in the peptide of interest (assuming that the first two amino acids cannot retain deuterons) (Bai et al. 1993). For PPARγ LBD, the deuterium recovery of a fully deuterated sample [(m(F) – m(N)) / MaxD] was averaged at 68%.

References

Baerga-Ortiz, A., Hughes, C.A., Mandell, J.G., and Komives, E.A. 2002. Epitope mapping of a monoclonal antibody against human thrombin by H/D-exchange mass spectrometry reveals selection of a diverse sequence in a highly conserved protein. *Protein Sci.* **11:** 1300–1308.

Bai, Y., Milne, J.S., Mayne, L.C., and Englander, S.W. 1993. Primary structure effects on peptide group hydrogen exchange. *Proteins* **17:** 75–86.

Berger, J.P., Petro, A.E., Macnaul, K.L., Kelly, L.J., Zhang, B.B., Richards, K., Elbrecht, A., Johnson, B.A., Zhou, G., Doebber, T.W., et al. 2003. Distinct properties and advantages of a novel peroxisome proliferator-activated protein γ selective modulator. *Mol. Endocrinol.* **17:** 662–676.

Brown, K.K., Henke, B.R., Blanchard, S.G., Cobb, J.E., Mook, R., Kaldor, I., Kliewer, S.A., Lehmann, J.M., Lenhard, J.M., Harrington, W.W., et al. 1999. A novel N-aryl tyrosine activator of peroxisome proliferator-activated receptor-γ reverses the diabetic phenotype of the Zucker diabetic fatty rat. *Diabetes* **48:** 1415–1424.

Brzozowski, A.M., Pike, A.C., Dauter, Z., Hubbard, R.E., Bonn, T., Engstrom, O., Ohman, L., Greene, G.L., Gustafsson, J.A., and Carlquist, M. 1997. Molecular basis of agonism and antagonism in the oestrogen receptor. *Nature* **389:** 753–758.

Davidson, W., Frego, L., Peet, G.W., Kroe, R.R., Labadia, M.E., Lukas, S.M., Snow, R.J., Jakes, S., Grygon, C.A., Pargellis, C., et al. 2004. Discovery and characterization of a substrate selective p38α inhibitor. *Biochemistry* **43:** 11658–11671.

Ehring, H. 1999. Hydrogen exchange/electrospray ionization mass spectrometry studies of structural features of proteins and protein/protein interactions. *Anal. Biochem.* **267:** 252–259.

Engen, J.R. and Smith, D.L. 2001. Investigating protein structure and dynamics by hydrogen exchange MS. *Anal. Chem.* **73:** 256A–265A.

Englander, J.J., Del Mar, C., Li, W., Englander, S.W., Kim, J.S., Stranz, D.D., Hamuro, Y., and Woods Jr., V.L. 2003. Protein structure change studied by hydrogen-deuterium exchange, functional labeling, and mass spectrometry. *Proc. Natl. Acad. Sci.* **100:** 7057–7062.

Englander, S.W. and Kallenbach, N.R. 1984. Hydrogen exchange and structural dynamics of proteins and nucleic acids. *Q. Rev. Biophys.* **16:** 521–655.

Farnegardh, M., Bonn, T., Sun, S., Ljunggren, J., Ahola, H., Wilhelmsson, A., Gustafsson, J.A., and Carlquist, M. 2003. The three-dimensional structure of the liver X receptor β reveals a flexible ligand-binding pocket that can accommodate fundamentally different ligands. *J. Biol. Chem.* **278:** 38821–38828.

Gampe Jr., R.T., Montana, V.G., Lambert, M.H., Miller, A.B., Bledsoe, R.K., Milburn, M.V., Kliewer, S.A., Willson, T.M., and Xu, H.E. 2000. Asymmetry in the PPARgamma/RXRalpha crystal structure reveals the molecular basis of heterodimerization among nuclear receptors. *Mol. Cell* **5:** 545–555.

Hamuro, Y., Wong, L., Shaffer, J., Kim, J.S., Stranz, D.D., Jennings, P.A., Woods Jr., V.L., and Adams, J.A. 2002. Phosphorylation-driven motions in the COOH-terminal Src kinase, Csk, revealed through enhanced hydrogen-deuterium exchange and mass spectrometric studies (DXMS). *J. Mol. Biol.* **323:** 871–881.

Hamuro, Y., Coales, S.J., Southern, M.R., Nemeth-Cawley, J.F., Stranz, D.D., and Griffin, P.R. 2003. Rapid analysis of protein structure and dynamics by hydrogen/deuterium exchange mass spectrometry. *J. Biomol. Tech.* **14:** 171–182.

Hoofnagle, A.N., Resing, K.A., Goldsmith, E.J., and Ahn, N.G. 2001. Changes in protein conformational mobility upon activation of extracellular regulated protein kinase-2 as detected by hydrogen exchange. *Proc. Natl. Acad. Sci.* **98:** 956–961.

Johnson, B.A., Wilson, E.M., Li, Y., Moller, D.E., Smith, R.G., and Zhou, G. 2000. Ligand-induced stabilization of PPARγ monitored by NMR spectroscopy: Implications for nuclear receptor activation. *J. Mol. Biol.* **298:** 187–194.

Kallenberger, B.C., Love, J.D., Chatterjee, V.K., and Schwabe, J.W. 2003. A dynamic mechanism of nuclear receptor activation and its perturbation in a human disease. *Nat. Struct. Biol.* **10:** 136–140.

Kauppi, B., Jakob, C., Farnegardh, M., Yang, J., Ahola, H., Alarcon, M., Calles, K., Engstrom, O., Harlan, J., Muchmore, S., et al. 2003. The three-dimensional structures of antagonistic and agonistic forms of the glucocorticoid receptor ligand-binding domain: RU-486 induces a transconformation that leads to active antagonism. *J. Biol. Chem.* **278:** 22748–22754.

Kossiakoff, A.A. 1982. Protein dynamics investigated by the neutron diffraction-hydrogen exchange technique. *Nature* **296:** 713–721.

Leesnitzer, L.M., Parks, D.J., Bledsoe, R.K., Cobb, J.E., Collins, J.L., Consler, T.G., Davis, R.G., Hull-Ryde, E.A., Lenhard, J.M., Patel, L., et al. 2002. Functional consequences of cysteine modification in the ligand binding sites of peroxisome proliferator activated receptors by GW9662. *Biochemistry* **41:** 6640–6650.

Mangelsdorf, D.J., Thummel, C., Beato, M., Herrlich, P., Schutz, G., Umesono, K., Blumberg, B., Kastner, P., Mark, M., Chambon, P., et al. 1995. The nuclear receptor superfamily: The second decade. *Cell* **83:** 835–839.

Nagy, L. and Schwabe, J.W. 2004. Mechanism of the nuclear receptor molecular switch. *Trends Biochem. Sci.* **29:** 317–324.

Nolte, R.T., Wisely, G.B., Westin, S., Cobb, J.E., Lambert, M.H., Kurokawa, R., Rosenfeld, M.G., Willson, T.M., Glass, C.K., and Milburn, M.V. 1998. Ligand binding and co-activator assembly of the peroxisome proliferator-activated receptor-γ. *Nature* **395:** 137–143.

Oberfield, J.L., Collins, J.L., Holmes, C.P., Goreham, D.M., Cooper, J.P., Cobb, J.E., Lenhard, J.M., Hull-Ryde, E.A., Mohr, C.P., Blanchard, S.G., et al. 1999. A peroxisome proliferator-activated receptor gamma ligand inhibits adipocyte differentiation. *Proc. Natl. Acad. Sci.* **96:** 6102–6106.

Olefsky, J.M. and Saltiel, A.R. 2000. PPARγ and the treatment of insulin resistance. *Trends Endocrinol. Metab.* **11:** 362–368.

Pike, A.C., Brzozowski, A.M., Hubbard, R.E., Bonn, T., Thorsell, A.G., Engstrom, O., Ljunggren, J., Gustafsson, J.A., and Carlquist, M. 1999. Structure of the ligand-binding domain of oestrogen receptor beta in the presence of a partial agonist and a full antagonist. *EMBO J.* **18:** 4608–4618.

Pissios, P., Tzameli, I., Kushner, P., and Moore, D.D. 2000. Dynamic stabilization of nuclear receptor ligand binding domains by hormone or corepressor binding. *Mol. Cell* **6:** 245–253.

Saltiel, A.R. 2001. New perspectives into the molecular pathogenesis and treatment of type 2 diabetes. *Cell* **104:** 517–529.

Schwabe, J.W. and Teichmann, S.A. 2004. Nuclear receptors: The evolution of diversity. *Sci. STKE* **2004:** pe4.

Willson, T.M., Brown, P.J., Sternbach, D.D., and Henke, B.R. 2000. The PPARs: From orphan receptors to drug discovery. *J. Med. Chem.* **43:** 527–550.

Wright, P.E. and Dyson, H.J. 1999. Intrinsically unstructured proteins: Re-assessing the protein structure–function paradigm. *J. Mol. Biol.* **293:** 321–331.

Yan, X., Broderick, D., Leid, M.E., Schimerlik, M.I., and Deinzer, M.L. 2004. Dynamics and ligand-induced solvent accessibility changes in human retinoid X receptor homodimer determined by hydrogen deuterium exchange and mass spectrometry. *Biochemistry* **43:** 909–917.

Yang, W., Rachez, C., and Freedman, L.P. 2000. Discrete roles for peroxisome proliferator-activated receptor γ and retinoid X receptor in recruiting nuclear receptor coactivators. *Mol. Cell. Biol.* **20:** 8008–8017.

Zhang, Z. and Smith, D.L. 1993. Determination of amide hydrogen exchange by mass spectrometry: A new tool for protein structure elucidation. *Protein Sci.* **2:** 522–531.

Zhang, Z., Post, C.B., and Smith, D.L. 1996. Amide hydrogen exchange determined by mass spectrometry: Application to rabbit muscle aldolase. *Biochemistry* **35:** 779–791.